Chapter 2
Conformal Dynamics Interlude

Abstract We have seen that models of dynamical breaking of the electroweak symmetry are theoretically appealing and constitute one of the best motivated natural extensions of the standard model. These are also among the most challenging models to work with since they require deep knowledge of gauge dynamics in a regime where perturbation theory fails. In particular, it is of utmost importance to gain information on the nonperturbative dynamics of non-abelian four dimensional gauge theories. In this chapter we elucidate the physics of non-Abelian gauge theories as function of the gauge group, number of flavors, colors and matter representation.

2.1 Phases of Gauge Theories

Non-abelian gauge theories exist in a number of distinct phases which can be classified according to the characteristic dependence of the potential energy on the distance between two well separated static sources. The collection of all of these different behaviors, when represented, for example, in the flavor-color space, constitutes the *phase diagram* of the given gauge theory. The phase diagram of $SU(N)$ gauge theories as functions of number of the gauge group, flavors, colors and matter representation has been investigated in [1–14].

The analytical tools we will use for such an exploration are: (i) Precise results from higher order perturbation theory [14–16]; (ii) The conjectured all orders beta function for nonsupersymmetric gauge theories with fermionic matter in arbitrary representations of the gauge group [4, 6]; (ii) The truncated Schwinger-Dyson equation (SD) [17–19] (referred also as the ladder approximation in the literature).

We wish to study the phase diagram of any asymptotically free nonsupersymmetric theories with fermionic matter transforming according to a generic representation of an SU(N) gauge group as function of the number of colors and flavors.

F. Sannino, *Dynamical Stabilization of the Fermi Scale*, SpringerBriefs in Physics,
DOI: 10.1007/978-3-642-33341-5_2, © The Author(s) 2013

We start by characterizing the possible phases via the potential $V(r)$ between two electric test charges separated by a large distance r. The list of possible potentials is given below:

$$\textbf{Coulomb}: \quad V(r) \propto \frac{1}{r} \tag{2.1}$$

$$\textbf{Free electric}: \quad V(r) \propto \frac{1}{r\log(r)} \tag{2.2}$$

$$\textbf{Free magnetic}: \quad V(r) \propto \frac{\log(r)}{r} \tag{2.3}$$

$$\textbf{Higgs}: \quad V(r) \propto \text{constant} \tag{2.4}$$

$$\textbf{Confining}: \quad V(r) \propto \sigma r\,. \tag{2.5}$$

A nice review of these phases can be found in [20] which here we reconsider for completeness. In the Coulomb phase, the electric charge $e^2(r)$ is a constant while in the free electric phase massless electrically charged fields renormalize the charge to zero at long distances as, i.e. $e^2(r) \sim 1/\log(r)$. QED is an abelian example of a free electric phase. The free magnetic phase occurs when massless magnetic monopoles renormalize the electric coupling constant at large distance with $e^2(r) \sim \log(r)$.

In the Higgs phase, the condensate of an electrically charged field gives a mass gap to the gauge fields by the Anderson-Higgs-Kibble mechanism and screens electric charges, leading to a potential which, up to an additive constant, has an exponential Yukawa decay to zero at long distances. In the confining phase, there is a mass gap with electric flux confined into a thin tube, leading to the linear potential with string tension σ.

We will be mainly interested in finding theories possessing a non-Abelian Coulomb phase or being close in the parameter space to these theories. In this phase we have massless interacting quarks and gluons exhibiting the Coulomb potential. This phase occurs when there is a non-trivial, infrared fixed point of the renormalization group. These are thus non-trivial, interacting, four dimensional conformal field theories. In the Coulomb phase the situation is actually more involved since for strong electrical charges the nonperturbative physical spectrum is much more involved.

To guess the behavior of the magnetic charge, at large distance separation, between two test magnetic charges one uses the Dirac condition:

$$e(r)g(r) \sim 1\,. \tag{2.6}$$

Then it becomes clear that $g(r)$ is constant in the Coulomb phase, increases with $\log(r)$ in the free electric phase and decreases as $1/\log(r)$ in the free magnetic phase. In these three phases the potential goes like $g^2(r)/r$. A linearly rising potential in

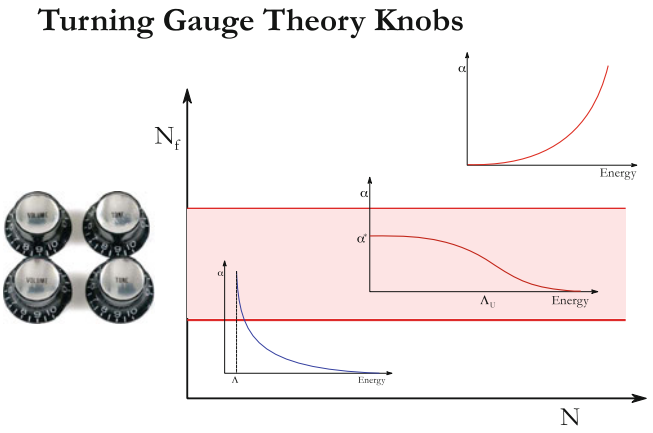

Fig. 2.1 A generic gauge theory has different Knobs one can tune. For example by changing the number of flavors one can enter in different phases. The *pink* region is the conformal region, i.e. the one where the coupling constant freezes at large distances (small energy). The region above the *pink* one corresponds to a non-abelian QED like theory and below to a QCD-like region. We have also plotted the cartoon of the running of the various coupling constants in the regions away from the boundaries of the conformal window. The *diagram* above is the qualitative one expected for a gauge theory with matter in the adjoint representation

the Higgs phase for magnetic test charges corresponds to the Meissner effect in the electric charges.

Confinement does not survive the presence of massless matter in the fundamental representation, such as light quarks in QCD. This is so since it is more convenient for the underlying theory to pop from the vacuum virtual quark-antiquark pairs when pulling two electric test charges apart. The potential for the confining phase will then change and there is no distinction between Higgs and confining phase.

Under electric-magnetic duality one exchanges electrically charged fields with magnetic ones then the behavior in the free electric phase is mapped in that of the free magnetic phase. The Higgs and confining phases are also expected to be exchanged under duality. Confinement can then be understood as the dual Meissner effect associated with a condensate of monopoles.

There is one more phase to consider which occurs when a given gauge theory at very high energies reaches an ultraviolet fixed point. The theory, in this case, is said to be asymptotically safe. Although there is not rigorous proof Weinberg [21] speculated that even the properly quantum corrected gravitational theory might develop such an ultraviolet fixed point which would *save* gravity from invalidating itself at and above the Planck scale. We refer to [22] for an up-to-date review and a list of relevant references on the subject (Fig. 2.1).

2.2 UV and IR Fixed Points of Gauge Theories at the Four Loops and Beyond

To gain a quantitative analytic understanding of the phase structure of different gauge theories we investigate the zeros of the perturbative beta function to the maximum known order and for one of the zeros also the limit of large number of flavors to all-orders.

We consider the perturbative expression of the beta function and the fermion mass anomalous dimension for a generic gauge theory with only fermionic matter in the $\overline{\text{MS}}$ scheme to four loops which was derived in [23, 24]:

$$\frac{da}{d\ln\mu^2} = \beta(a) = -\beta_0 a^2 - \beta_1 a^3 - \beta_2 a^4 - \beta_3 a^5 + O(a^6)\,, \tag{2.7}$$

$$-\frac{d\ln m}{d\ln\mu^2} = \frac{\gamma(a)}{2} = \gamma_0 a + \gamma_1 a^2 + \gamma_2 a^3 + \gamma_3 a^4 + O(a^5)\,, \tag{2.8}$$

where $m = m(\mu^2)$ is the renormalized (running) fermion mass and μ is the renormalization point in the $\overline{\text{MS}}$ scheme and $a = \alpha/4\pi = g^2/16\pi^2$ where $g = g(\mu^2)$ is the renormalized coupling constant of the theory.

The explicit expression of the coefficients above are reported in the Appendix A.2 for completeness. Note also that the beta function is gauge independent, order by order in perturbation theory [23]. The same also holds for the anomalous dimension of the fermion mass γ.

Here we report the investigation of the structure of the zeros of the four-loops beta function for any matter representation and gauge group [11, 15, 16]. Interestingly in [15] we found a *universal* classification of the behavior of the zeros as function of the number of flavors n_f.

To exemplify the various possible topologies emerging to this order, we plot the real nontrivial zeros as function of the number of flavors normalized to the one above which asymptotic freedom is lost ($\overline{n}_f$) in Fig. 2.2. The solid black lines represent the location of the ultraviolet (UV) zeros while the red-ones to the infrared (IR) stable fixed points, and finally the shaded areas are the regions where the β function is positive. To help visualizing the different regions the vertical axis is rescaled [15] according to the function $a^* = 2\arctan(5a)/\pi$, mapping $[-\infty, +\infty]$ into the interval $[-1, 1]$.

A straight vertical line corresponds to a fixed value of n_f and the intersection of this line with the solid curves determines the number of the zeros, the color of the curves the type of zeros (if red is IR and if black is UV), and finally the corresponding horizontal value is the coupling location. The landscape of the zeros was termed *zerology* in [15].

We investigated also the negative values of α since this is the most natural mathematical setting. In fact, the properties of the pure Yang-Mills theory at negative

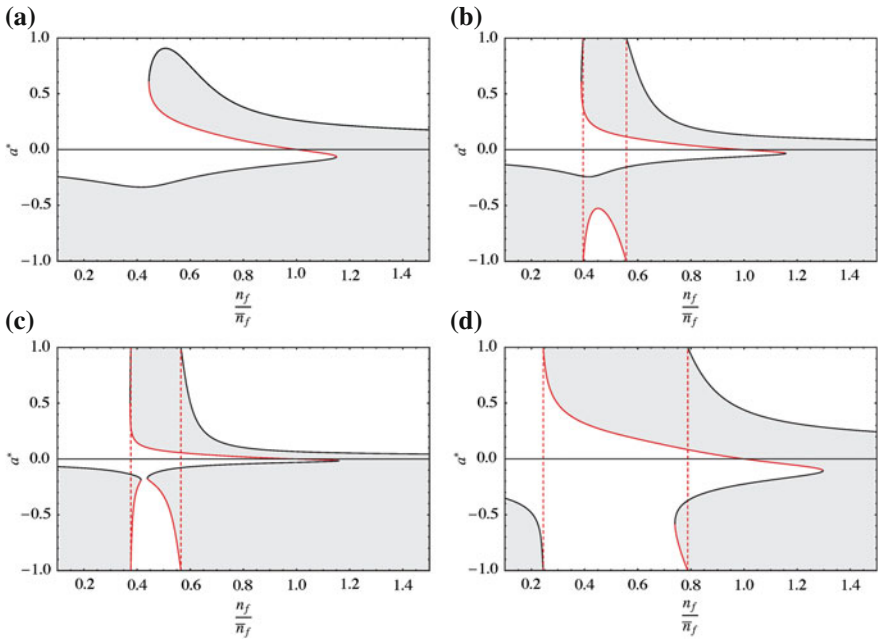

Fig. 2.2 The four different topologies displayed above classify the entire *zerology* landscape. We show, in each plot, the regions of positive (*gray*) and negative (*white*) values of the beta function for different gauge theories. The *solid lines*, per each figure, are the locations of the zeros of the beta functions. The *lines* of UV fixed points are in *black* while the IR ones in *red*. We have defined $a^* = \frac{2}{\pi} \arctan(5a)$. The *vertical dashed red-lines* correspond to the location where one zero approaches infinity: **a** first kind of topology, **b** second kind of topology, **c** third kind of topology, **d** fourth kind of topology

α were studied on the lattice by Li and Meurice in [25] showing interesting relations between the positive and negative regions of α.

By explicit enumeration [15] it is possible to identify just four distinct topologies covering the full available zerology for any gauge group and matter representation reported in Fig. 2.2.

The four-loop analysis tells us that [15]:

- At small number of flavors there is only a negative ultraviolet zero.
- At around and above $\overline{n}_f$ we observe the existence of three zeros, two ultraviolets and one infrared. The infrared one, near $\overline{n}_f$, is the Banks-Zaks [26] point. Above $\overline{n}_f$, the IR fixed point is now at a negative value of α and at a new critical number of flavors collides with the UV fixed point zero at a negative value of the coupling, forming a double zero. At this point the beta function is positive for any negative alpha.

- At very large number of flavors the UV fixed point, for positive values of alpha, always exists and approaches zero asymptotically as $n_f^{-2/3}$. The explicit derivation is provided in Sect. 2.4.3.
- By increasing n_f from zero there is always a critical number of flavors above which an IR fixed point emerges for positive α.

The distinguishing feature of different topologies is how the zeros merge or disappear as function of n_f.

The topology A (Fig. 2.2a) is characterized by the fact that the zeros always remain at finite values of the coupling. This means that when a zero disappear it has to annihilate with another one. This happens at two distinct locations. One at a positive value of the coupling and the other at a negative one occurring after asymptotic freedom is lost.

In the topology B, represented in Fig. 2.2b, as for the previous case, we still observe the merging of the IR and UV zeros at two different number of flavors. In this case, however, there is a region in the number of flavors, where the UV fixed point located at positive couplings reaches infinity at finite n_f and appears on the negative axis as an IR fixed point. The region where the new IR fixed point appears (on the negative coupling constant axis) ends before asymptotic freedom is lost.

The defining feature shown in Fig. 2.2c for topology C is that the appearance of two more merging points at negative values of α.

In Fig. 2.2d, topology D, one observes that the IR zero at a positive value of the coupling reachers infinity at a finite value of the number of flavors, which is the distinctive feature of this topology.

A new feature at the four-loop order is that two positive nontrivial zeros, one IR and the other UV, can emerge simultaneously and can annihilate at a particular value of n_f. At the two-loop level this feature does not exist and, in particular, no nontrivial ultraviolet fixed point is seen.

As an example where these topologies arise we consider $SU(N)$ with fundamental fermions as function of N. For $N = 2$ and 3 the topology A occurs. Increasing N the maximum value reached by the positive UV zero increases and for $N = 4$ it reaches infinity and therefore it enters topology B. Increasing N further the local maximum of the IR negative zero-curve increases till it pinches the UV negative zero line for $N = 11$ entering topology C. Topology D is not realized in this case. On the other hand any $SU(N)$ gauge theory with $N \geq 2$ fermions and fermions in the adjoint representation lead to topology D.

In Table 2.1 we provide a catalogue of the four-loop zerology for $SU(N)$, $SO(N)$ and $SP(2N)$ gauge theories with fermions transforming according to the fundamental and the 2-index representations.

Table 2.1 Catalogue of the four-loop zerology for $SU(N)$, $SO(N)$ and $SP(2N)$ gauge theories with fermions transforming according to the fundamental and the 2-index representations

Rep.	Top. A	Top. B	Top. C	Top. D
$SU(N)$				
FUND	$N = 2, 3$	$4 \leq N \leq 11$	$N \geq 12$	–
ADJ	–	–	–	$N \geq 2$
2-SYM	–	–	–	$N \geq 2$
2-ASY	$N = 3, 4, 5$	$N = 6, 7$	$8 \leq N \leq 26$	$N \geq 27$
$SO(N)$				
FUND	–	$N \leq 6$	$N = 5$	$N = 3, 4$
ADJ	–	–	–	$N \geq 3$
2-SYM	–	–	–	$N \geq 3$
$SP(2N)$				
FUND	$N = 1, 2$	$3 \leq N \leq 4$	$N \geq 5$	–
ADJ	–	–	–	$N \geq 1$
2-ASY	$N = 3, 4$	$N = 2, 5$	$6 \leq N \leq 14$	$N \geq 15$

2.3 Conformal Window

The conformal window is defined as the region in theory space, as function of number of flavors and colors where the underlying gauge theory displays large distance conformality for a positive value of the coupling α. $\overline{n}_f$ constitutes the upper boundary of the conformal window and the lower boundary here is estimated by identifying for which number of flavors the theory looses the infrared fixed point at a given number of colors. Several methods have been used to constrain the conformal window for non-supersymmetric gauge theories. We will review only a few here which has been proven to be useful either to guide lattice simulations or that have been shown effective in producing relevant physical quantities.

2.4 Four-Loop Conformal Window

Having at our disposal the four-loops beta function we use it to estimate the lower boundary of the conformal window. However, due to the fact that it is obviously a truncated beta function the true window can be quantitatively different.

The results for the $SU(N)$ gauge groups are presented in Fig. 2.3 for the fundamental, two-index symmetric, two-index antisymmetric and adjoint representation. The conformal window at the four-loop level is considerably wider, for any representation, when compared with the Schwinger-Dyson results [1, 2] or the one obtained using the critical number of flavors where the free energy changes sign, as suggested in [11]. For completeness the conformal window for the orthogonal and symplectic

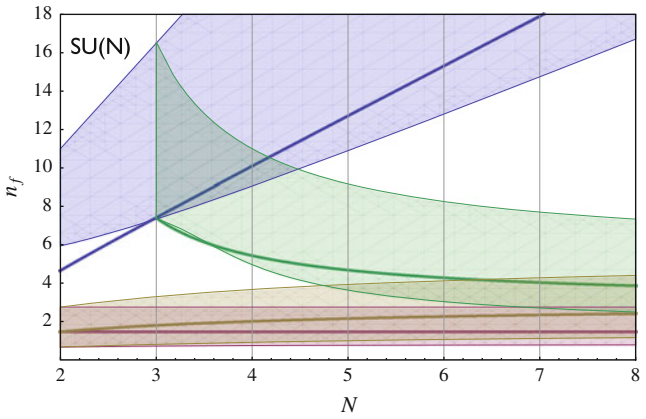

Fig. 2.3 Conformal window for $SU(N)$ groups for the fundamental representation (*upper light-blue*), two-index antisymmetric (next to the *highest light-green*), two-index symmetric (third window from the *top light-brown*) and finally the adjoint representation (*bottom light-pink*). The lower boundary corresponds to the point where the infrared fixed point disappears at four loops. The *solid thick lines* correspond to the number of flavors for which the all-orders beta function predicts an anomalous dimension equal to unity

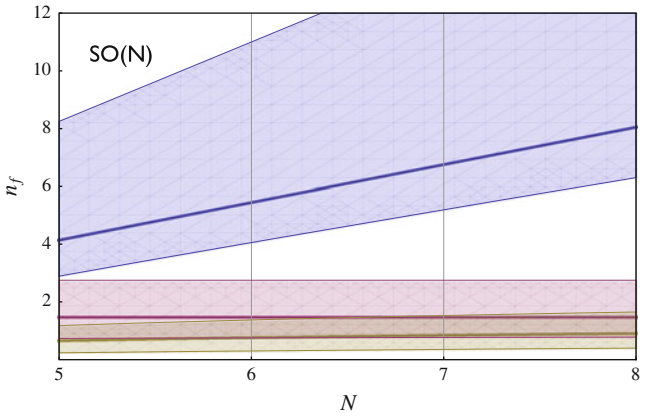

Fig. 2.4 Conformal window for $SO(N)$ groups for the fundamental representation (*upper light-blue*), two-index antisymmetric (which is the adjoint and second from the top (*pink*-region)), two-index symmetric (bottom window in *light-brown*)

gauge groups is also shown respectively in Figs. 2.4 and 2.5. There is a universal trend towards the widening of the conformal regions with respect to earlier estimates using other nonperturbative methods.

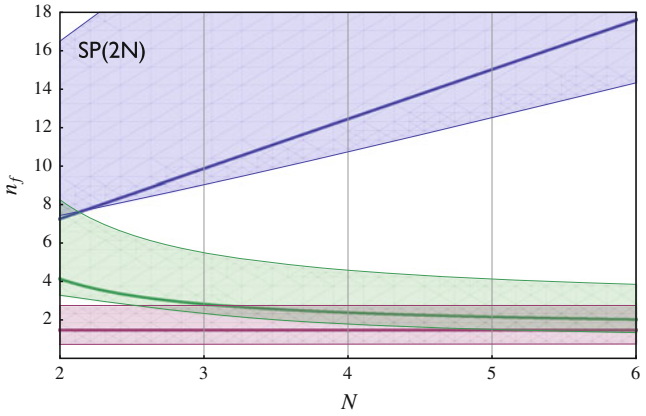

Fig. 2.5 Conformal window for $SP(2N)$ groups for the fundamental representation (*upper light-blue*), two-index antisymmetric (next to the *highest light-green*), two-index symmetric, i.e. the adjoint, (bottom window in *light-pink*)

2.4.1 All-Orders Beta Function Comparison

We have recently argued for the existence of a scheme in which an all-orders beta function [6] assumes the form:

$$\frac{\beta(a)}{a} = -\frac{a}{3}\frac{11C_2(G) - 2T(r)\,n_f\,(2 + \Delta_F\gamma)}{1 - 2a\frac{17}{11}C_2(G)}\,, \tag{2.9}$$

with

$$\Delta_F = 1 + \frac{7}{11}\frac{C_2(G)}{C_2(r)}\,. \tag{2.10}$$

The group invariants defined in Appendix A.2. The *scheme independent* analytical expression of the anomalous dimension of the mass at the IR positive zero is:

$$\gamma = \frac{11C_2(G) - 4T(r)n_f}{2n_f T(r)\left(1 + \frac{7}{11}\frac{C_2(G)}{C_2(r)}\right)}\,. \tag{2.11}$$

We plot, for reference, in Figs. 2.3, 2.4 and 2.5 the lines corresponding to this anomalous dimension equal to unity. These are the solid thick curves for the different representations. These lines could be viewed as the lower boundary of the conformal window if it is marked by the anomalous dimension to be unity. The size of these regions are consistent with the ones derived via gauge dualities in [27, 28].

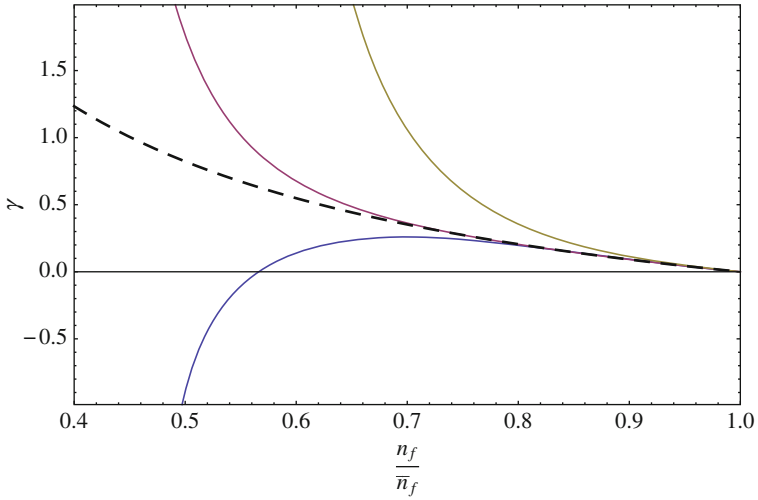

Fig. 2.6 Anomalous dimension of the mass, at the infrared fixed point, for $SU(3)$ as function of the number of fundamental flavors at two loops (*upper brown-curve*), three-loops (second *curve* from the top in *magenta*), all-orders (*dashed-curve* in *black*), four-loops (*bottom curve* in *blue*)

2.4.2 Four-Loop Anomalous Dimensions

In Fig. 2.6 we plot the anomalous dimension of the mass for the $SU(3)$ gauge theory, as function of the number of fundamental flavors, at the IR fixed point as derived in [15, 16]. The three solid lines correspond respectively, from top to bottom, to the two-, three- and four-loop results. Of course, perturbation theory is reliable only in a small range of flavors near $\overline{n}_f$. A similar behavior is observed for any other gauge group, matter representation and different number of colors.

Having at hand an all-order scheme-independent result, we compare it with the perturbative one. The dashed line, in Fig. 2.6, is the all-order anomalous dimension from Eq. (2.11). It is striking that the all-order result is much more well behaved than the four-loop predictions which, in this example, reach large and negative values long before loosing the IR positive zero.

Due to the phenomenological interest in models of minimal walking technicolor [1, 29, 30] we report the anomalous dimension at the fixed point also for the $SU(2)$ gauge theory with two-adjoint fermions in Fig. 2.7. These theories are being subject to intensive numerical investigations via lattice simulations [31–59].

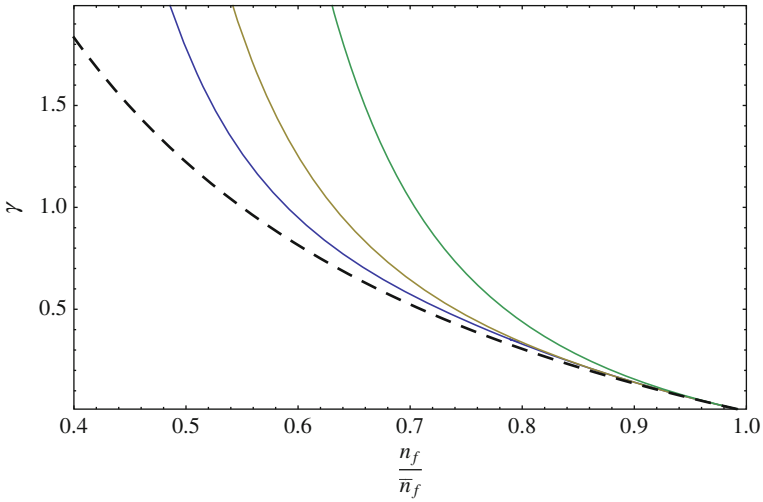

Fig. 2.7 Anomalous dimension of the mass, at the infrared fixed point, for $SU(2)$ as function of the number of adjoint Dirac flavors at two loops (*up green-curve*), three-loops (second *curve* from the *top*), four-loops (third *curve* in *blue*), all-orders (*dashed curve* in *black*)

2.4.3 Asymptotic Safety at Large n_f: A New Phase

To the four-loop order a positive UV zero appears for a sufficiently large number of flavors. We observed that the value of the zero as function of number of flavors decreases monotonically as $n_f^{-2/3}$ at four loops. In fact, it is possible to generalize this behavior to any finite order in perturbation theory. Consider the equation for the zeros of the beta function in which the leading powers in the number of flavors are made explicit:

$$b_0 n_f + \sum_{k=1}^{\infty} b_k \, n_f^k \, \alpha^k = 0 \,, \tag{2.12}$$

where $b_0 = \beta_0/n_f$ and $b_k = \beta_k/n_f^k$. We used the fact that the first and second coefficient of the beta function are linear in the number of flavors and, in general, the successive coefficients have one extra power of n_f [60]. Therefore the coefficients b_k are finite at large number of flavors.

We define:

$$x = n_f \alpha \,, \tag{2.13}$$

and the equation at any fixed perturbative order P reads:

$$b_0 n_f + \sum_{k=1}^{P} b_k \, x^k = 0 \,. \tag{2.14}$$

At large n_f the solution approaches:

$$x = \left(-\frac{b_0 n_f}{b_P}\right)^{\frac{1}{P}} \longrightarrow \alpha = \left(-\frac{b_0}{b_P}\right)^{\frac{1}{P}} n_f{}^{\frac{1-P}{P}} . \tag{2.15}$$

There are P complex solutions for x lying on a circle in the complex plane. A positive solution exists only if b_P is positive at large n_f. This is indeed the case, at the four-loop order, for any gauge theory showing that the UV positive zero vanishes as $n_f^{-2/3}$. If this UV zero persists to higher orders its location will change albeit will vanish faster as a function of n_f when increasing P, i.e. the exponent $(1-P)/P$ increases in absolute value. The case $n_f^{-2/3}$ is recovered for $P = 3$.

Interestingly it is possible to sum exactly the perturbative infinite sum for the beta function, at large of number of flavors given that the leading coefficients are known. The result is:

$$\frac{3}{4n_f T_F}\frac{\beta(a)}{a^2} = 1 + \frac{H(x)}{n_f} + \mathcal{O}\left(n_f^{-2}\right) . \tag{2.16}$$

The explicit form of $H(x)$ can be found in [60]. The important feature, here, is that $H(x)$ possesses a negative singularity at $x = 3\pi/T_F$. This demonstrates that there always is a solution for the existence of a nontrivial UV fixed point at the leading order in n_f for the following positive value of the coupling:

$$\alpha_{\rm UV} = \frac{3\pi}{T_F n_f} . \tag{2.17}$$

The function $H(x)$ has also other singularities which might signal the presence of new zeros which we will not consider here, but that would be worth exploring.

Higher order terms in n_f^{-1} can, in principle, modify the result if the singularity structure is such to remove or modify its location.

A more complete discussion of the singularity structure of the coefficients of the n_f^{-1} expansion has appeared in [60] also for QED. It seems plausible that the smallest UV fixed point is an all-orders feature.

2.4.4 Schwinger-Dyson in the Rainbow Approximation

For nonsupersymmetric theories an old way to get quantitative estimates is to use the *rainbow* approximation to the Schwinger-Dyson equation [61, 62], see Fig. 2.8. Here the full nonperturbative fermion propagator in momentum space reads

$$iS^{-1}(p) = Z(p)\left(\not{p} - \Sigma(p)\right) , \tag{2.18}$$

and the Euclidianized gap equation in Landau gauge is given by

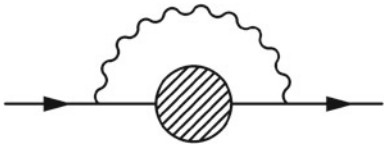

Fig. 2.8 Rainbow approximation for the fermion self energy function. The boson is a gluon

$$\Sigma(p) = 3C_2(r) \int \frac{d^4k}{(2\pi)^4} \frac{\alpha\left((k-p)^2\right)}{(k-p)^2} \frac{\Sigma(k^2)}{Z(k^2)k^2 + \Sigma^2(k^2)}\,, \tag{2.19}$$

where $Z(k^2) = 1$ in the Landau gauge and we linearize the equation by neglecting $\Sigma^2(k^2)$ in the denominator. Upon converting it into a differential equation and assuming that the coupling $\alpha(\mu) \approx \alpha_c$ is varying slowly ($\beta(\alpha) \simeq 0$) one gets the approximate (WKB) solutions

$$\Sigma(p) \propto p^{-\gamma(\mu)}, \qquad \Sigma(p) \propto p^{\gamma(\mu)-2}\,. \tag{2.20}$$

The critical coupling is given in terms of the quadratic Casimir of the representation of the fermions

$$\alpha_c \equiv \frac{\pi}{3C_2(r)}\,. \tag{2.21}$$

The anomalous dimension of the fermion mass operator is

$$\gamma(\mu) = 1 - \sqrt{1 - \frac{\alpha(\mu)}{\alpha_c}} \sim \frac{3C_2(r)\alpha(\mu)}{2\pi}\,. \tag{2.22}$$

The first solution corresponds to the running of an ordinary mass term (*hard* mass) of nondynamical origin and the second solution to a *soft* mass dynamically generated. In fact in the second case one observes the $1/p^2$ behavior in the limit of large momentum.

Within this approximation spontaneous symmetry breaking occurs when α reaches the critical coupling α_c given in Eq. (2.21). From Eq. (2.22) it is clear that α_c is reached when γ is of order unity [17, 18, 63]. Hence the symmetry breaking occurs when the soft and the hard mass terms scale as function of the energy scale in the same way. In Ref. [17], it was noted that in the lowest (ladder) order, the gap equation leads to the condition $\gamma(2-\gamma) = 1$ for chiral symmetry breaking to occur. To all orders in perturbation theory this condition is gauge invariant and also equivalent nonperturbatively to the condition $\gamma = 1$. However, to any finite order in perturbation theory these conditions are, of course, different. Interestingly the condition $\gamma(2-\gamma) = 1$ leads again to the critical coupling α_c when using the perturbative leading order expression for the anomalous dimension which is $\gamma = \frac{3C_2(r)}{2\pi}\alpha$.

To summarize, the idea behind this method is simple. One simply compares the two couplings in the infrared associated to (i) an infrared zero in the β function, call it α^* with (ii) the critical coupling, denoted with α_c, above which a dynamical mass for the fermions generates nonperturbatively and chiral symmetry breaking occurs. If α^*

is less than α_c chiral symmetry does not occur and the theory remains conformal in the infrared, viceversa if α^* is larger than α_c then the fermions acquire a dynamical mass and the theory cannot be conformal in the infrared. The condition $\alpha^* = \alpha_c$ provides the desired $n_f^{\rm SD}$ as function of N. In practice to estimate α^* one uses the two-loop beta function while the truncated SD equation to determine α_c as we have done before. This corresponds to when the anomalous dimension of the quark mass operator becomes approximately unity.

The two-loop fixed point value of the coupling constant is:

$$\frac{\alpha^*}{4\pi} = -\frac{\beta_0}{\beta_1}. \tag{2.23}$$

with the following definition of the two-loop beta function

$$\beta(g) = -\frac{\beta_0}{(4\pi)^2} g^3 - \frac{\beta_1}{(4\pi)^4} g^5 \,, \tag{2.24}$$

where g is the gauge coupling and the beta function coefficients are given by

$$\beta_0 = \frac{11}{3} C_2(G) - \frac{4}{3} T(r) n_f \tag{2.25}$$

$$\beta_1 = \frac{34}{3} C_2^2(G) - \frac{20}{3} C_2(G) T(r) n_f - 4 C_2(r) T(r) n_f \,. \tag{2.26}$$

To this order the two coefficients are universal, i.e. do not depend on which renormalization group scheme one has used to determine them. The perturbative expression for the anomalous dimension reads:

$$\gamma(g^2) = \frac{3}{2} C_2(r) \frac{g^2}{4\pi^2} + O(g^4) \,. \tag{2.27}$$

with $\gamma = -d \ln m / d \ln \mu$ and m the renormalized fermion mass.

For a fixed number of colors the critical number of flavors for which the order of α^* and α_c changes is defined by imposing $\alpha^* = \alpha_c$, and it is given by

$$n_f^{\rm SD} = \frac{17 C_2(G) + 66 C_2(r)}{10 C_2(G) + 30 C_2(r)} \frac{C_2(G)}{T(r)} \,. \tag{2.28}$$

Comparing with the previous results obtained using the four-loop approximation or the conjectured all orders beta function the striking differences is that the anomalous dimension of the fermion mass operator, for the same number of flavors, is typically overestimated by the SD analysis while the conformal window is smaller, i.e. critical number of flavors is predicted to be higher than other methods.

2.5 Gauge Duals and Conformal Window

One of the most fascinating possibilities is that generic asymptotically free gauge theories have magnetic duals. In fact, in the late nineties, in a series of ground breaking papers Seiberg [64, 65] provided strong support for the existence of a consistent picture of such a duality within a supersymmetric framework. Supersymmetry is, however, quite special and the existence of such a duality does not automatically imply the existence of nonsupersymmetric duals. One of the most relevant results put forward by Seiberg has been the identification of the boundary of the conformal window for supersymmetric QCD as function of the number of flavors and colors. The dual theories proposed by Seiberg pass a set of mathematical consistency relations known as 't Hooft anomaly conditions (in [66]). Another important tool has been the knowledge of the all orders supersymmetric beta function [67–69].

Arguably the existence of a possible dual of a generic nonsupersymmetric asymptotically free gauge theory able to reproduce its infrared dynamics must match the 't Hooft anomaly conditions [66].

We have exhibited several solutions of these conditions for QCD in [27] and for certain gauge theories with higher dimensional representations in [28]. An earlier exploration already appeared in the literature [70]. The novelty with respect to these earlier results are: (i) The request that the gauge singlet operators associated to the magnetic baryons should be interpreted as bound states of ordinary baryons [27]; (ii) The fact that the asymptotically free condition for the dual theory matches the lower bound on the conformal window obtained using the all orders beta function [4]. These extra constraints help restricting further the number of possible gauge duals without diminishing the exactness of the associate solutions with respect to the 't Hooft anomaly conditions.

We will briefly summarize here the novel solutions to the 't Hooft anomaly conditions for QCD and the theories with higher dimensional representations. The resulting *magnetic* dual allows to predict the critical number of flavors above which the asymptotically free theory, in the electric variables, enters the conformal regime as predicted using the all orders conjectured beta function [4].

2.5.1 QCD Duals

The underlying gauge group is $SU(3)$ while the quantum flavor group is

$$SU_L(n_f) \times SU_R(n_f) \times U_V(1)\,, \tag{2.29}$$

and the classical $U_A(1)$ symmetry is destroyed at the quantum level by the Adler-Bell-Jackiw anomaly. We indicate with $Q^i_{\alpha;c}$ the two component left spinor where $\alpha = 1, 2$ is the spinor index, $c = 1, \ldots, 3$ is the color index while $i = 1, \ldots, n_f$ represents

Table 2.2 Field content of an SU(3) gauge theory with quantum global symmetry $SU_L(n_f) \times SU_R(n_f) \times U_V(1)$

Fields	$[SU(3)]$	$SU_L(n_f)$	$SU_R(n_f)$	$U_V(1)$
Q	$\square$	$\square$	1	1
$\widetilde{Q}$	$\overline{\square}$	1	$\overline{\square}$	-1
G_μ	Adj	1	1	1

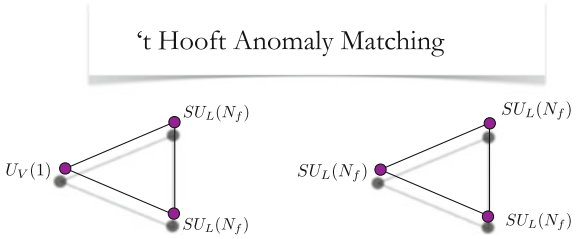

Fig. 2.9 The 't Hooft anomaly matching conditions are related to the saturation of the global anomalies stemming out of the one-loop triangle diagrams represented, for the theory of interest, here. According to 't Hooft both theories, i.e. the electric and the magnetic ones, should yield the same global anomalies

the flavor. $\widetilde{Q}_i^{\alpha;c}$ is the two component conjugated right spinor. We summarize the transformation properties in Table 2.2.

The global anomalies are associated to the triangle diagrams featuring at the vertices three $SU(n_f)$ generators (either all right or all left), or two $SU(n_f)$ generators (all right or all left) and one $U_V(1)$ charge. We indicate these anomalies for short with:

$$SU_{L/R}(n_f)^3\,, \qquad SU_{L/R}(n_f)^2\ U_V(1)\,. \tag{2.30}$$

For a vector like theory there are no further global anomalies (Fig. 2.9). The cubic anomaly factor, for fermions in fundamental representations, is 1 for Q and -1 for $\tilde{Q}$ while the quadratic anomaly factor is 1 for both leading to

$$SU_{L/R}(n_f)^3 \propto \pm 3\,, \quad SU_{L/R}(n_f)^2 U_V(1) \propto \pm 3\,. \tag{2.31}$$

If a magnetic dual of QCD does exist one expects it to be weakly coupled near the critical number of flavors below which one breaks large distance conformality in the electric variables. This idea is depicted in Fig 2.10.

Determining a possible unique dual theory for QCD is, however, not simple given the few mathematical constraints at our disposal, as already observed in [70]. The saturation of the global anomalies is an important tool but is not able to select out a unique solution. We shall see, however, that one of the solutions, when interpreted as the QCD dual, leads to a prediction of a critical number of flavors corresponding exactly to the one obtained via the conjectured all orders beta function.

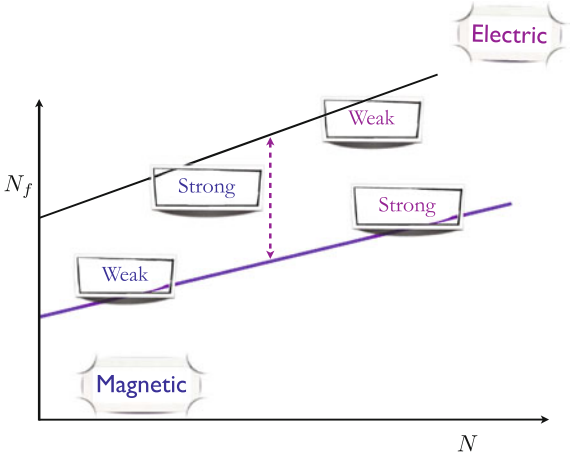

Fig. 2.10 Schematic representation of the phase diagram as function of number of flavors and colors. For a given number of colors by increasing the number flavors within the conformal window we move from the *lowest line* (*violet*) to the *upper* (*black*) one. The *upper black line* corresponds to the one where one looses asymptotic freedom in the electric variables and the *lower line* where chiral symmetry breaks and long distance conformality is lost. In the *magnetic* variables the situation is reverted and the perturbative line, i.e. the one where one looses asymptotic freedom in the magnetic variables, correspond to the one where chiral symmetry breaks in the electric ones

We seek solutions of the anomaly matching conditions for a gauge theory $SU(X)$ with global symmetry group $SU_L(n_f)\times SU_R(n_f)\times U_V(1)$ featuring *magnetic* quarks q and $\widetilde{q}$ together with $SU(X)$ gauge singlet states identifiable as baryons built out of the *electric* quarks Q. Since mesons do not affect directly global anomaly matching conditions we could add them to the spectrum of the dual theory. We study the case in which X is a linear combination of number of flavors and colors of the type $\alpha n_f + 3\beta$ with α and β integer numbers.

We add to the *magnetic* quarks gauge singlet Weyl fermions which can be identified with the baryons of QCD but massless. The generic dual spectrum is summarized in Table 2.3.

The wave functions for the gauge singlet fields A, C and S are obtained by projecting the flavor indices of the following operator

$$\varepsilon^{c_1 c_2 c_3} Q^{i_1}_{c_1} Q^{i_2}_{c_2} Q^{i_3}_{c_3} , \tag{2.32}$$

over the three irreducible representations of $SU_L(n_f)$ as indicated in the Table 2.3. These states are all singlets under the $SU_R(n_f)$ flavor group. Similarly one can construct the only right-transforming baryons $\widetilde{A}$, $\widetilde{C}$ and $\widetilde{S}$ via $\widetilde{Q}$. The B states are made by two Q fields and one right field $\overline{\widetilde{Q}}$ while the D fields are made by one Q and two $\overline{\widetilde{Q}}$ fermions. y is the, yet to be determined, baryon charge of the *magnetic* quarks while the baryon charge of composite states is fixed in units of the QCD quark one.

Table 2.3 Massless spectrum of *magnetic* quarks and baryons and their transformation properties under the global symmetry group

Fields	$[SU(X)]$	$SU_L(n_f)$	$SU_R(n_f)$	$U_V(1)$	# of copies
q	$\square$	$\square$	1	y	1
$\widetilde{q}$	$\overline{\square}$	1	$\overline{\square}$	$-y$	1
A	1	$\begin{array}{l}\square\\\square\end{array}$	1	3	ℓ_A
S	1	$\square\square$	1	3	ℓ_S
C	1	$\begin{array}{ll}\square&\square\\\square&\end{array}$	1	3	ℓ_C
B_A	1	$\begin{array}{l}\square\\\square\end{array}$	$\square$	3	ℓ_{B_A}
B_S	1	$\square\square$	$\square$	3	ℓ_{B_S}
D_A	1	$\square$	$\begin{array}{l}\square\\\square\end{array}$	3	ℓ_{D_A}
D_S	1	$\square$	$\square\square$	3	ℓ_{D_S}
$\widetilde{A}$	1	1	$\begin{array}{l}\overline{\square}\\\square\\\square\end{array}$	-3	$\ell_{\widetilde{A}}$
$\widetilde{S}$	1	1	$\overline{\square\square\square}$	-3	$\ell_{\widetilde{S}}$
$\widetilde{C}$	1	1	$\begin{array}{ll}\overline{\square}&\overline{\square}\\\square&\end{array}$	-3	$\ell_{\widetilde{C}}$

The last column represents the multiplicity of each state and each state is a Weyl fermion

The ℓs count the number of times the same baryonic matter representation appears as part of the spectrum of the theory. Invariance under parity and charge conjugation of the underlying theory requires $\ell_J = \ell_{\widetilde{J}}$ with $J = A, S, \ldots, C$ and $\ell_B = -\ell_D$.

Having defined the possible massless matter content of the gauge theory dual to QCD we compute the $SU_L(n_f)^3$ and $SU_L(n_f)^2\, U_{V(1)}$ global anomalies in terms of the new fields:

$$\begin{aligned} SU_L(n_f)^3 \propto X &+ \frac{(n_f-3)(n_f-6)}{2}\,\ell_A \\ &+ \frac{(n_f+3)(n_f+6)}{2}\,\ell_S + (n_f^2-9)\,\ell_C \\ &+ (n_f-4)n_f\,\ell_{B_A} + (n_f+4)n_f\,\ell_{B_S} + \frac{n_f(n_f-1)}{2}\,\ell_{D_A} \\ &+ \frac{n_f(n_f+1)}{2}\,\ell_{D_S} = 3\,, \end{aligned} \tag{2.33}$$

$$\begin{aligned} SU_L(n_f)^2\; U_V(1) \propto y\,X &+ 3\frac{(n_f-3)(n_f-2)}{2}\,\ell_A \\ &+ 3\frac{(n_f+3)(n_f+2)}{2}\,\ell_S + 3(n_f^2-3)\,\ell_C \\ &+ 3(n_f-2)n_f\,\ell_{B_A} + 3(n_f+2)n_f\,\ell_{B_S} + 3\frac{n_f(n_f-1)}{2}\,\ell_{D_A} \\ &+ 3\frac{n_f(n_f+1)}{2}\,\ell_{D_S} = 3\,. \end{aligned} \tag{2.34}$$

The right-hand side is the corresponding value of the anomaly for QCD.

Table 2.4 Massless spectrum of *magnetic* quarks and baryons and their transformation properties under the global symmetry group

Fields	$[SU(2n_f - 5N)]$	$SU_L(n_f)$	$SU_R(n_f)$	$U_V(1)$	# of copies
q	$\square$	$\square$	1	$\frac{N(2n_f-5)}{2n_f-5N}$	1
$\widetilde{q}$	$\overline{\square}$	1	$\overline{\square}$	$-\frac{N(2n_f-5)}{2n_f-5N}$	1
A	1	$\begin{array}{l}\square\\\square\end{array}$	1	3	2
B_A	1	$\begin{array}{l}\square\square\\\square\end{array}$	$\square$	3	-2
D_A	1	$\square$	$\begin{array}{l}\square\square\\\square\end{array}$	3	2
$\widetilde{A}$	1	1	$\begin{array}{l}\overline{\square}\\\overline{\square}\\\square\end{array}$	-3	2

The last column represents the multiplicity of each state and each state is a Weyl fermion

2.5.2 A Realistic QCD Dual

We have found several solutions to the anomaly matching conditions presented above. Some were found previously in [70]. Here we start with a new solution in which the gauge group is $SU(2n_f - 5N)$ with the number of colors N equal to 3. It is, however, convenient to keep the dependence on N explicit.

The solution above corresponds to the following value assumed by the indices and y baryonic charge in Table 2.4.

$$\begin{aligned} &X = 2n_f - 5N, \quad \ell_A = 2\,, \quad \ell_{D_A} = -\ell_{B_A} = 2\,, \\ &\ell_S = \ell_{B_S} = \ell_{D_S} = \ell_C = 0\,, \quad y = N\,\frac{2n_f - 5}{2n_f - 15}\,, \end{aligned} \tag{2.35}$$

with $N = 3$. X must assume a value strictly larger than one otherwise it is an abelian gauge theory. This provides the first nontrivial bound on the number of flavors:

$$n_f > \frac{5N + 1}{2}\,, \tag{2.36}$$

which for $N = 3$ requires $n_f > 8$.

2.5.3 Conformal Window from the Dual Magnetic Theory

Asymptotic freedom of the newly found theory is dictated by the coefficient of the one-loop beta function:

$$\beta_0 = \frac{11}{3}(2n_f - 5N) - \frac{2}{3}n_f \,. \tag{2.37}$$

To this order in perturbation theory the gauge singlet states do not affect the magnetic quark sector and we can hence determine the number of flavors obtained by requiring the dual theory to be asymptotic free. i.e.:

$$n_f \geq \frac{11}{4}N = 2.75 \qquad \text{Dual Asymptotic Freedom} \,. \tag{2.38}$$

Quite remarkably this value is close to the one predicted by means of the all orders conjectured beta function for the lowest bound of the conformal window, in the *electric* variables, when taking the anomalous dimension of the mass to be $\gamma = 1$. I.e. at large N[1]

$$n_f^{BF}|_{\gamma=1} \simeq 2.57N \,. \tag{2.39}$$

For N = 3 duality would seem to require the critical number of flavors to be 8.25.[2] We consider this a nontrivial and interesting result.

To investigate the decoupling of each flavor at the time one needs to introduce bosonic degrees of freedom. These are not constrained by anomaly matching conditions. Interactions among the mesonic degrees of freedom and the fermions in the dual theory cannot be neglected in the regime when the dynamics is strong. The simplest mesonic operator M_i^j transforming simultaneously according to the antifundamental representation of $SU_L(n_f)$ and the fundamental representation of $SU_R(n_f)$ leads to the following type of interactions for the dual theory:

$$\begin{aligned} L_{\rm M} = {} & Y_{q\tilde{q}}\; q\; M\; \widetilde{q} + Y_{AB_A}\; AM\overline{B}_A + Y_{CB_A}\; CM\overline{B}_A \\ & + Y_{CB_S}\; C\, M\overline{B}_S + Y_{SB_S}\; SM\overline{B}_S \\ & + Y_{B_AD_A} B_A M\overline{D}_A + Y_{B_AD_S}\; B_A\, M\overline{D}_S \\ & + Y_{B_SD_A} B_S M\overline{D}_A + Y_{B_SD_S} B_S M\overline{D}_S + \text{h.c.} \end{aligned} \tag{2.40}$$

The coefficients of the various operators are matrices taking into account the multiplicity with which each state occurs. The number of operators drastically reduces if we consider only the ones linear in M. The dual quarks and baryons interact via mesonic exchanges. We have considered only the meson field for the bosonic spectrum because it is the one with the most obvious interpretation in terms on the electric variables. One can also envision adding new scalars charged under the dual gauge group [70] and in this case one can have contact interactions between the magnetic quarks and baryons. We expect these operators to play a role near the lower bound of the conformal window of the magnetic theory where QCD is expected to become free. It is straightforward to adapt the terms above to any anomaly matching solution.

[1] This result differs from the one found in the original paper [27] and reported in the earlier review [71] because, in the meanwhile, the all-orders beta function was corrected in [6].

[2] Actually given that X must be at least 2 we must have $n_f \geq 8.5$ rather than 8.25.

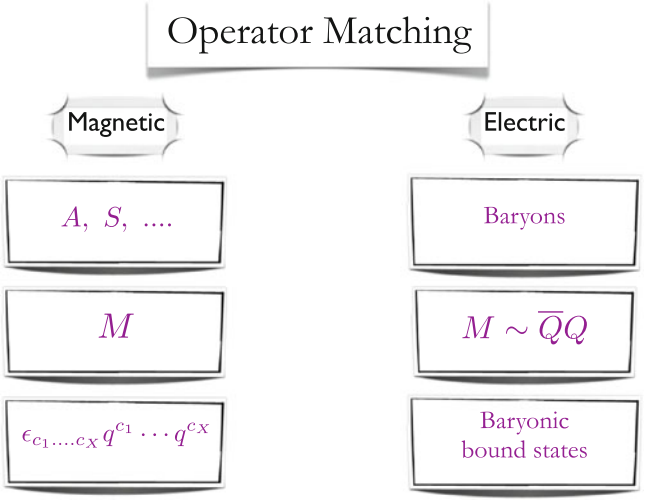

Fig. 2.11 We propose the above correspondence between the gauge singlet operators of the magnetic theory and the electric ones. The novelty introduced in [27] with respect to any of the earlier approaches is the identification of the *magnetic* baryons, i.e. the ones constructed via the magnetic quarks, with bound states of baryons in the electric variables

In Seiberg's analysis it was also possible to match some of the operators of the magnetic theory with the ones of the electric theory. The situation for QCD is, in principle, more involved although it is clear that certain magnetic operators match exactly the respective ones in the electric variables. These are the meson M and the massless baryons, $A, \widetilde{A}, \ldots, S$ shown in Table 2.3. The baryonic type operators constructed via the magnetic dual quarks have baryonic charge which is a multiple of the ordinary baryons and, hence, we propose to identify them, in the electric variables, with bound states of QCD baryons. We summarize the proposed operator matching constraints in Fig. 2.11.

The generalization to a generic number of colors is currently under investigation. It is an interesting issue and to address it requires the knowledge of the spectrum of baryons for arbitrary number of colors. It is reasonable to expect, however, a possible nontrivial generalization to any number of odd colors[3]. A relevant application of gauge duality has been to determine the left-right vector two-point function correlator at the lower boundary of the conformal window [72].

2.6 Walking Versus Jumping Dynamics

We concentrated our efforts mostly on the size of the conformal window neglecting, almost entirely, what happens at the boundary between the conformally intact phase and the broken one. However, despite much efforts we do not yet know the physical

[3] For an even number of colors the baryons are bosons and a the analysis must modify.

properties at the boundary between a conformally broken and a conformally restored phase for generic gauge theories. This problem remains an important mystery to solve. A famous conjecture has been put forward some time ago [19, 73] and it is known as Miransky scaling. In [74] it was argued for the potential existence of another intriguing possibility leading to a radically different near-conformal behavior. For setting up the stage we start with a brief review of the Miransky scaling and modeling. Following [74] we then introduce the alternative scenario and deduce the consequences for models of dynamical electroweak symmetry breaking.

2.6.1 Miransky Scaling and Walking Dynamics

This scaling arises under the following assumptions: (i) A given gauge theory possesses simultaneously, at least, a non-trivial infrared (IR) fixed point and an ultraviolet (UV) one; (ii) Upon changing an external parameter of the theory, e.g. the number of flavors, at a critical value of this parameter the IR fixed point merges with the UV fixed point; (iii) This merging is sufficiently smooth that the nearby conformal phase is felt, in the conformally broken phase, for values of the external parameter near the phase transition.

Without loss of generality it is possible to model the beta function near the critical number of flavors as follows:

$$\beta_{MY} = -\alpha^2 \left(\alpha - 1 - \sqrt{\delta}\right) \left(\alpha - 1 + \sqrt{\delta}\right) = -\alpha^2((\alpha - 1)^2 - \delta)\,. \tag{2.41}$$

The double zero at the origin embodies asymptotic freedom and $\delta = n_f - n_f^c$. For positive values of δ the beta function possesses a non-trivial IR and UV fixed point at the following values of the coupling:

$$\alpha_{IR} = 1 - \sqrt{\delta}, \qquad \text{and} \qquad \alpha_{UV} = 1 + \sqrt{\delta}\,. \tag{2.42}$$

At $n_f = n_f^c$ the fixed points merge and for $n_f < n_f^c$ the beta function looses the non-trivial fixed points. For negative δ within the following range:

$$-\frac{1}{8} < \delta \leq 0 \tag{2.43}$$

there is a global maximum of the beta function at the origin, a local minimum at $\alpha = \frac{1}{4}(3 - \sqrt{1 + 8\delta})$ and a local maximum at $\alpha = \frac{1}{4}(3 + \sqrt{1 + 8\delta})$. For illustration we plot the beta function for different values of δ in Fig. 2.12. It is possible to find an analytical solution to the RG equation:

$$d \ln \mu = \frac{d\alpha}{\beta_{MY}}\,, \tag{2.44}$$

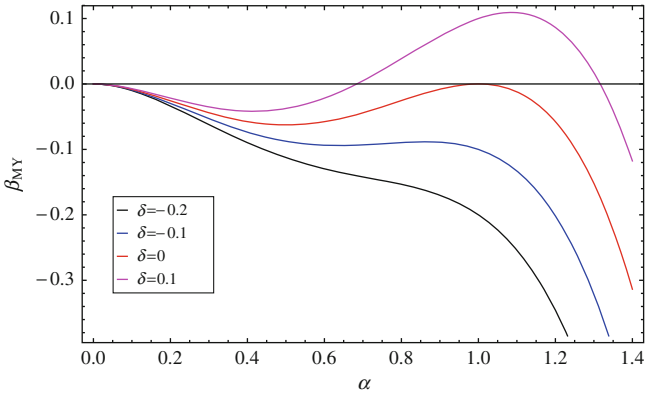

Fig. 2.12 β_{MY} for different values of $\delta = n_f - n_f^c$

reading:

$$\ln \frac{\mu}{\mu_0} = \frac{\alpha(1+\delta)\text{ArcTanh}\left[\frac{-1+\alpha}{\sqrt{\delta}}\right] + \sqrt{\delta}\left(1-\delta+\alpha\ln\left[\frac{(\alpha-1)^2-\delta}{\alpha^2}\right]\right)}{\alpha(-1+\delta)^2\sqrt{\delta}}\Bigg|_{\alpha(\mu_0)}^{\alpha(\mu)}. \tag{2.45}$$

If we were to consider the case of δ positive, but smaller than unity so that asymptotic freedom is kept, we would discover that there are three distinct branches. The one to the left of the IR fixed point, the one where α is in between the nontrivial IR and UV fixed point, and the one to the right of the nontrivial UV fixed point. To the left of the IR fixed point one starts the flow from any μ_0 sufficiently close to the trivial UV fixed point and one ends up at the attractive IR fixed point. Another *asymptotically safe* theory is defined in between the two non-trivial fixed points. In this region the coupling runs at low energies to the IR fixed point and raises at high energies till the non-trivial UV fixed point is reached. Finally, to the right of the non-trivial UV fixed point the theory, and hence beta function, runs in the deep infrared to increasingly large values of the coupling.

We turn now our attention to negative values of δ corresponding to the phase in which the beta function features no non-trivial fixed points. To elucidate the near-conformal dynamics we investigate the region $-1/8 < \delta < 0$. In particular we will consider the limit $-\delta = n_f^c - n_f \to 0$. In the deep infrared the coupling constant runs to infinity and we start the running in the UV near $\alpha = 1$ at μ_0. With these boundary conditions we find:

$$\Lambda_{MY} = \frac{\mu_0}{n_f^c - n_f} \exp\left[-\frac{\pi}{2\sqrt{n_f^c - n_f}}\right], \; n_f \to n_f^c, n_f \leq n_f^c\,. \tag{2.46}$$

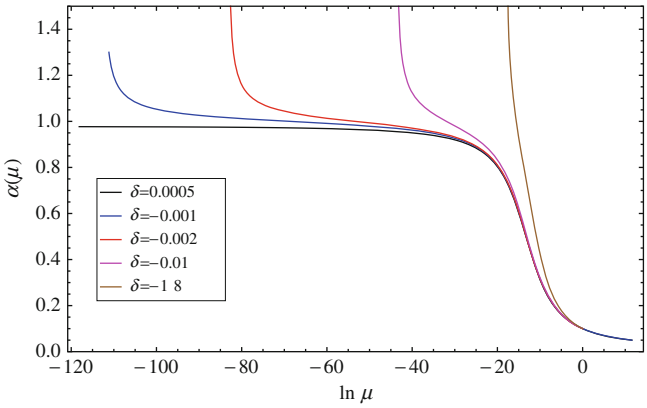

Fig. 2.13 Running of the coupling constant coming from β_{MY} for different values of $\delta = n_f - n_f^c$ within the *walking* regime. All the solutions are normalized at μ_0 such that $\alpha(\mu_0) = 0.1$ and μ is normalized to μ_0

Here Λ_{MY} is the infrared scale to be identified, for example, with a physical scale of the theory such as the mass of a hadron. This scale vanishes exponentially fast when approaching the critical number of flavors above which the infrared fixed point is generated. This exponential behavior is the essence of the Miransky scaling.

In Fig. 2.13 we plot the running of the coupling constant for different negative values of δ with the normalization condition $\alpha(\mu_0) = 0.1$. The figure visualizes the idea of walking dynamics introduced by Holdom [75, 76] and further crystallized in [63, 77]. In lay terms the coupling constant runs slowly, i.e. *walks*, towards the infrared value remaining near constant over a range of energies becoming wider and wider as one approaches, as function of δ, the double fixed point. Further assuming that the beta function corresponds to an underlying gauge theory featuring fermions we now determine the scaling behavior of the chiral condensate of the theory in the walking regime. Defining with γ the anomalous dimension of the mass of the Dirac fermion Q in a given representation of an underlying gauge group we have the following well-known RG equation:

$$\begin{aligned}\langle \bar{Q}Q\rangle_\mu &= \exp\left(\int_\Lambda^\mu \mathrm{d}(\ln\mu)\gamma(\alpha(\mu))\right)\langle \bar{Q}Q\rangle_\Lambda \\ &= \exp\left(\int_{\alpha(\Lambda)}^{\alpha(\mu)} \mathrm{d}\alpha\,\frac{\gamma(\alpha)}{\beta(\alpha)}\right)\langle \bar{Q}Q\rangle_\Lambda \end{aligned} \tag{2.47}$$

relating the condensate at two different energies. Using β_{MY} case in the walking region we have

$$\langle \bar{Q}Q\rangle_\mu = \exp\left(\int_{\alpha(\Lambda)}^{\alpha(\mu)} d\alpha \frac{\gamma(\alpha)}{-\alpha^2((\alpha-1)^2+|\delta|)}\right)\langle \bar{Q}Q\rangle_\Lambda$$
$$\simeq \exp\left(\gamma(1)\int_{\alpha(\Lambda)}^{\alpha(\mu)} d\alpha \frac{1}{\beta_{MY}}\right)\langle \bar{Q}Q\rangle_\Lambda = \left(\frac{\mu}{\Lambda}\right)^{\gamma(1)}\langle \bar{Q}Q\rangle_\Lambda . \quad (2.48)$$

In the last passage we have used the definition of the beta function and, in the first step, assumed that the anomalous dimension of the mass operator is smooth across the phase transition. $\gamma(1) = \gamma(\alpha_{IR} = \alpha_{UV})$ is the value of the anomalous dimension at the merger. We have re-derived the power-law enhancement of the chiral condensate with the energy distinctive of walking dynamics. Since γ is evaluated at the fixed point its value is scheme-independent [6]. If we further model $\gamma = \alpha$ we have$\gamma(\alpha_{IR/UV}) = 1 \mp \sqrt{\delta}$, with $\gamma(\alpha_{IR}) + \gamma(\alpha_{UV}) = 2$.

2.6.2 *Jumping Dynamics*

The previous section embodies the standard paradigm of walking dynamics. However this picture is far from established analytically or via first principle lattice simulations in four dimensions, while lower dimensional examples exist [78]. It is therefore relevant to consider other theoretical scenarios and their impact on particle physics phenomenology. We start by observing that there is the logical possibility that the full beta function of the theory develops, at least, a zero in the denominator. This occurs exactly for supersymmetric gauge theories [67] and the all-orders beta function conjectured to be valid also for non-supersymmetric gauge theories with fermionic matter [4, 6]. Moreover it is reasonable to expect that the full perturbative and non-perturbative contributions to the beta function conspire to generate a non-trivial pole structure [79]. Whatever the pole structure is, if the underlying theory displays conformality, there will be also zeros in the numerator of the beta function associated to the non-trivial fixed point structure of the theory. Here we consider the simplest example in which the beta function has a simple nontrivial zero in the numerator and a simple pole. We will always assume the existence of the trivial double zero at the origin so that the beta function contains information about the asymptotically free nature of the theory. Without loss of generality we write:

$$\beta_{Jump} = -\alpha^2 \frac{1-\delta-\alpha}{1-\alpha} . \quad (2.49)$$

By construction this beta function has a zero in the numerator for any δ which is to the left of the pole value $\alpha_{pole} = 1$ for δ positive and to the right for δ negative. Here we take again $\delta = n_f - n_f^c$. It is straightforward to show that this zero corresponds

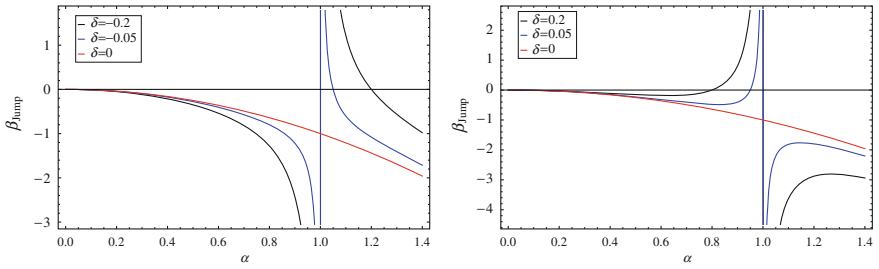

Fig. 2.14 β_{Jump} for different values of $\delta = n_f - n_f^c$

to an IR (UV) fixed point for $\delta > 0$ ($\delta < 0$):

$$\alpha_{IR(UV)} = 1 - \delta, \quad \delta > 0 \quad (\delta < 0) \quad \text{and} \quad |\delta| \leq 1\,. \tag{2.50}$$

Because of the presence of the pole the beta function describes two disconnected theories. One which is continuously connected to the asymptotically free underlying gauge theory and the other which is not. We plot the beta function for positive and negative values of delta in Fig. 2.14. At exactly $\delta = 0$ the numerator and denominator of the beta function cancel and we are left with $\beta_{Jump}^{\delta=0} = -\alpha^2$ which is the red curve in Fig. 2.14. What happens at the phase boundary? We will demonstrate that there is a sudden jump as we drop the number of flavors below the critical number of flavors (i.e. at $\delta = 0$) of the intrinsic physical scale of the theory.

We start by constructing the analytical solution for the RG equation of the coupling which reads:

$$\ln\frac{\mu}{\mu_0} = \frac{1}{\alpha(1-\delta)}\Big|_{\alpha(\mu_0)}^{\alpha(\mu)} + \frac{\delta}{(1-\delta)^2}\ln\left[\frac{1-\delta-\alpha}{\alpha}\right]\Big|_{\alpha(\mu_0)}^{\alpha(\mu)}. \tag{2.51}$$

Holding fixed, as done for the Miransky scaling case, the coupling constant at a given renormalization scale one observes that the newly generated scale increases with decreasing the number of flavors below the conformal window in the following way:

$$\Lambda_{Jump} = \Lambda_c\left[1 - (n_f^c - n_f)\ln\left(n_f^c - n_f\right)\right], n_f \to n_f^c, n_f \leq n_f^c\,. \tag{2.52}$$

$\Lambda_c = \mu_0 \exp\left[\frac{\ln\alpha_0}{\alpha_0}\right]$ is the renormalization group invariant scale of the theory at the critical number of flavors. However for $n_f > n_f^c$ no infrared scale is generated and necessarily there must be a *jump* in the spectrum from Λ_c to zero (Fig. 2.15). This result shows that β_{MY} and β_{Jump} describe two distinct physical systems. For illustration we summarize in Fig. 2.16 the behavior of the physical scale of the theory, as function of number of flavors, for Miransky scaling and jumping dynamics. To compare the two scaling laws we normalized the two scales at a given value of n_f.

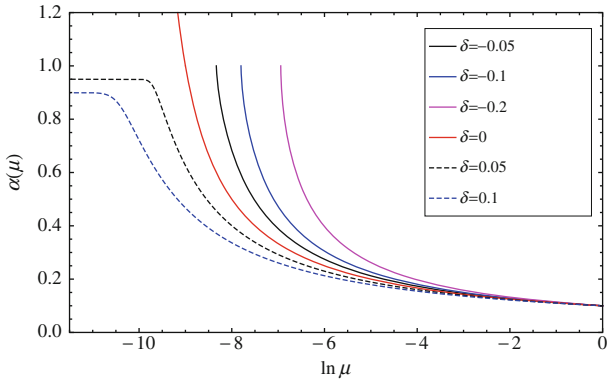

Fig. 2.15 Running of the coupling constant due to β_{Jump} for different values of $\delta = n_f - n_f^c$. All the solutions are normalized at μ_0 such that $\alpha(\mu_0) = 0.1$, and of course μ is normalized to μ_0

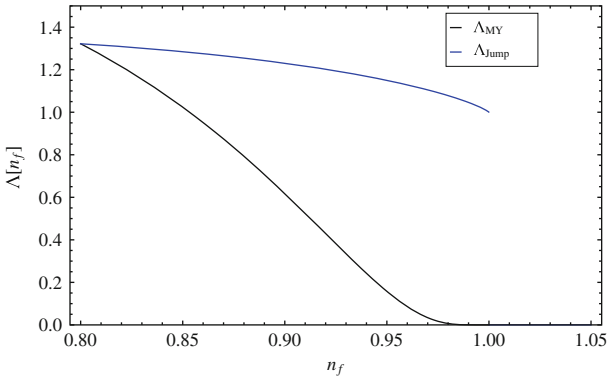

Fig. 2.16 Mass gap dependence on the number of flavors for the Miransky scaling (*lower black curve*) and for the jumping dynamics (*upper blue curve*). We have taken for illustration $n_f^c = 1$

Can jumping dynamics be used for models of dynamical electroweak symmetry breaking? At the conformal boundary the dynamics is QCD like and therefore one observes only a logarithmic enhancement of the condensate of the type $\langle \bar{Q}Q \rangle_\mu \simeq \gamma(1) \ln\left(\frac{\mu}{\Lambda}\right) \langle \bar{Q}Q \rangle_\Lambda$. The jumping dynamics does not lead to power-law enhancement of the chiral condensate required for *walking* technicolor. Furthermore the S-parameter in the jumping scenario automatically respects the lower bound put forward in [80] given that, opportunely normalized, at the phase boundary is as small as the one for QCD. Henceforth the answer to the original question is that one can break the electroweak theory via jumping dynamics but cannot accommodate the generation of the standard model fermion masses following the walking paradigm nor drastically reduce the QCD-like S-parameter.

We have shown that it is possible to devise a simple framework according to which the approach to the long distance conformality does not display any sign of walking

dynamics. All the current lattice investigations of the conformal window are not able to differentiate walking from jumping. The reasons being that: (i) The lattice results, for the moment, are performed for a fixed number of flavors and therefore either there is a nonzero infrared scale or the theory is conformal; (ii) The precise determination of the chiral condensate is not a simple task making harder to disentangle a power-law from a logarithmic enhancement of the condensate as function of the renormalization scale as well as the number of flavors; (iii) Even if the underlying dynamics is of walking type (with or without the introduction of four-fermion interactions) the extension of the region in the number of flavors and four-fermion coupling is not known and might be tiny; (iv) Measuring a large anomalous dimension of the mass is encouraging but alone insufficient to demonstrate the existence of walking dynamics.

Because of the discontinuity of the order parameter at the conformal phase transition, i.e. of the vacuum expectation value of the trace of the improved energy momentum tensor which is proportional to the intrinsic scale of the theory, jumping dynamics corresponds to a first order conformal phase transition. First order phase transitions are common in nature and therefore we expect jumping dynamics to constitute a likely scenario with inevitable important consequences on a large number of research fields ranging from a better understanding of strong dynamics and its holographic engineering to the construction of sensible extensions of the standard model.

References

1. F. Sannino, K. Tuominen, Phys. Rev. D **71**, 051901 (2005) [arXiv:hep-ph/0405209]
2. D.D. Dietrich, F. Sannino, Phys. Rev. D **75**, 085018 (2007) [arXiv:hep-ph/0611341]
3. T.A. Ryttov, F. Sannino, Phys. Rev. D **76**, 105004 (2007) [arXiv:0707.3166 [hep-th]]
4. T.A. Ryttov, F. Sannino, Phys. Rev. D **78**, 065001 (2008) [arXiv:0711.3745 [hep-th]]
5. F. Sannino, arXiv:0804.0182 [hep-ph]
6. C. Pica, F. Sannino, Phys. Rev. D **83**, 116001 (2011) [arXiv:1011.3832 [hep-ph]]
7. F. Sannino, Phys. Rev. D **72**, 125006 (2005) [hep-th/0507251]
8. F. Sannino, Phys. Rev. D **79**, 096007 (2009) [arXiv:0902.3494 [hep-ph]]
9. T.A. Ryttov, R. Shrock, Phys. Rev. D **81**, 116003 (2010) [Erratum-ibid. D **82**, 059903 (2010)] [arXiv:1006.0421 [hep-ph]]
10. N. Chen, T.A. Ryttov, R. Shrock, Phys. Rev. D **82**, 116006 (2010) [arXiv:1010.3736 [hep-ph]]
11. M. Mojaza, C. Pica, F. Sannino, Phys. Rev. D **82**, 116009 (2010) [arXiv:1010.4798 [hep-ph]]
12. O. Antipin, M. Mojaza, F. Sannino, Phys. Lett. B **712**, 119 (2012) [arXiv:1107.2932 [hep-ph]]
13. O. Antipin, S. Di Chiara, M. Mojaza, E. Molgaard, F. Sannino, arXiv:1205.6157 [hep-ph]
14. M. Mojaza, C. Pica, T.A. Ryttov, F. Sannino, arXiv:1206.2652 [hep-ph]
15. C. Pica, F. Sannino, Phys. Rev. D **83**, 035013 (2011) [arXiv:1011.5917 [hep-ph]]
16. T.A. Ryttov, R. Shrock, Phys. Rev. D **83**, 056011 (2011) [arXiv:1011.4542 [hep-ph]]
17. T. Appelquist, K.D. Lane, U. Mahanta, Phys. Rev. Lett. **61**, 1553 (1988)
18. A.G. Cohen, H. Georgi, Nucl. Phys. B **314**, 7 (1989)
19. V.A. Miransky, K. Yamawaki, Phys. Rev. D **55**, 5051 (1997) [Erratum-ibid. D **56**, 3768 (1997)] [arXiv:hep-th/9611142]
20. K.A. Intriligator, N. Seiberg, Nucl. Phys. Proc. Suppl. **45BC**, 1 (1996) [arXiv:hep-th/9509066]
21. S. Weinberg, Ultraviolet divergences in quantum theories of gravitation, in *General Relativity: An Einstein Centenary Survey*, ed. by S.W. Hawking, W. Israel (Cambridge University Press, Cambridge, 1979), p. 790

22. D.F. Litim, Phil. Trans. Roy. Soc. Lond. A **369**, 2759 (2011) [arXiv:1102.4624 [hep-th]]
23. T. van Ritbergen, J.A.M. Vermaseren, S.A. Larin, Phys. Lett. B **400**, 379 (1997) [hep-ph/9701390]
24. J.A.M. Vermaseren, S.A. Larin, T. van Ritbergen, Phys. Lett. B **405**, 327 (1997) [hep-ph/9703284]
25. L. Li, Y. Meurice, Phys. Rev. D **71**, 016008 (2005) [hep-lat/0410029]
26. T. Banks, A. Zaks, Nucl. Phys. B **196**, 189 (1982)
27. F. Sannino, Phys. Rev. D **80**, 065011 (2009) [arXiv:0907.1364 [hep-th]]
28. F. Sannino, arXiv:0909.4584 [hep-th]
29. D.K. Hong, S.D.H. Hsu, F. Sannino, Phys. Lett. B **597**, 89 (2004) [arXiv:hep-ph/0406200]
30. D.D. Dietrich, F. Sannino, K. Tuominen, Phys. Rev. D **72**, 055001 (2005) [arXiv:hep-ph/0505059]
31. S. Catterall, F. Sannino, Phys. Rev. D **76**, 034504 (2007) [arXiv:0705.1664 [hep-lat]]
32. L. Del Debbio, M.T. Frandsen, H. Panagopoulos, F. Sannino, JHEP **0806**, 007 (2008) [arXiv:0802.0891 [hep-lat]]
33. Y. Shamir, B. Svetitsky, T. DeGrand, Phys. Rev. D **78**, 031502 (2008) [arXiv:0803.1707 [hep-lat]]
34. A. Deuzeman, M.P. Lombardo, E. Pallante, Phys. Lett. B **670**, 41 (2008) [arXiv:0804.2905 [hep-lat]]
35. L. Del Debbio, A. Patella, C. Pica, Phys. Rev. D **81**, 094503 (2010) [arXiv:0805.2058 [hep-lat]]
36. S. Catterall, J. Giedt, F. Sannino, J. Schneible, JHEP **0811**, 009 (2008) [arXiv:0807.0792 [hep-lat]]
37. L. Del Debbio, A. Patella, C. Pica, PoS **LATTICE2008**, 064 (2008) [arXiv:0812.0570 [hep-lat]]
38. T. DeGrand, Y. Shamir, B. Svetitsky, Phys. Rev. D **79**, 034501 (2009) [arXiv:0812.1427 [hep-lat]]
39. A.J. Hietanen, J. Rantaharju, K. Rummukainen, K. Tuominen, JHEP **0905**, 025 (2009) [arXiv:0812.1467 [hep-lat]]
40. T. Appelquist, G.T. Fleming, E.T. Neil, Phys. Rev. D **79**, 076010 (2009) [arXiv:0901.3766 [hep-ph]]
41. A.J. Hietanen, K. Rummukainen, K. Tuominen, Phys. Rev. D **80**, 094504 (2009) [arXiv:0904.0864 [hep-lat]]
42. A. Deuzeman, M.P. Lombardo, E. Pallante, Phys. Rev. D **82**, 074503 (2010) [arXiv:0904.4662 [hep-ph]]
43. A. Hasenfratz, Phys. Rev. D **80**, 034505 (2009) [arXiv:0907.0919 [hep-lat]]
44. L. Del Debbio, B. Lucini, A. Patella, C. Pica, A. Rago, Phys. Rev. D **80**, 074507 (2009) [arXiv:0907.3896 [hep-lat]]
45. Z. Fodor, K. Holland, J. Kuti, D. Nogradi, C. Schroeder, Phys. Lett. B **681**, 353 (2009) [arXiv:0907.4562 [hep-lat]]
46. Z. Fodor, K. Holland, J. Kuti, D. Nogradi, C. Schroeder, JHEP **0911**, 103 (2009) [arXiv:0908.2466 [hep-lat]]
47. T. DeGrand, Phys. Rev. D **80**, 114507 (2009) [arXiv:0910.3072 [hep-lat]]
48. S. Catterall, J. Giedt, F. Sannino, J. Schneible, arXiv:0910.4387 [hep-lat]
49. F. Bursa, L. Del Debbio, L. Keegan, C. Pica, T. Pickup, Phys. Rev. D **81**, 014505 (2010) [arXiv:0910.4535 [hep-ph]]
50. E. Bilgici et al., Phys. Rev. D **80**, 034507 (2009) [arXiv:0902.3768 [hep-lat]]
51. J.B. Kogut, D.K. Sinclair, Phys. Rev. D **81**, 114507 (2010) [arXiv:1002.2988 [hep-lat]]
52. A. Hasenfratz, Phys. Rev. D **82**, 014506 (2010) [arXiv:1004.1004 [hep-lat]]
53. L. Del Debbio, B. Lucini, A. Patella, C. Pica, A. Rago, Phys. Rev. D **82**, 014509 (2010) [arXiv:1004.3197 [hep-lat]]
54. L. Del Debbio, B. Lucini, A. Patella, C. Pica, A. Rago, Phys. Rev. D **82**, 014510 (2010) [arXiv:1004.3206 [hep-lat]]

55. S. Catterall, L. Del Debbio, J. Giedt, L. Keegan, PoS **LATTICE2010**, 057 (2010) [arXiv:1010.5909 [hep-ph]]
56. Z. Fodor, K. Holland, J. Kuti, D. Nogradi, C. Schroeder, arXiv:1103.5998 [hep-lat]
57. R. Lewis, C. Pica, F. Sannino, Phys. Rev. D **85**, 014504 (2012) [arXiv:1109.3513 [hep-ph]]
58. Z. Fodor, K. Holland, J. Kuti, D. Nogradi, C. Schroeder, C.H. Wong, arXiv:1205.1878 [hep-lat]
59. J. Giedt, E. Weinberg, Phys. Rev. D **85**, 097503 (2012) [arXiv:1201.6262 [hep-lat]]
60. B. Holdom, Phys. Lett. B **694**, 74 (2010) [arXiv:1006.2119 [hep-ph]]
61. T. Maskawa, H. Nakajima, Prog. Theor. Phys. **52**, 1326 (1974)
62. R. Fukuda, T. Kugo, Nucl. Phys. B **117**, 250 (1976)
63. K. Yamawaki, M. Bando, K.i. Matumoto, Phys. Rev. Lett. **56**, 1335 (1986)
64. N. Seiberg, Phys. Rev. D **49**, 6857 (1994) [arXiv:hep-th/9402044]
65. N. Seiberg, Nucl. Phys. B **435**, 129 (1995) [arXiv:hep-th/9411149]
66. G. 't Hooft, C. Itzykson, A. Jaffe, H. Lehmann, P.K. Mitter, I.M. Singer, R. Stora (eds.), *Recent Developments in Gauge Theories*. Nato Advanced Study Institutes Series: Series B, Physics, vol. 59 (Plenum, New York, 1980), p. 438
67. V.A. Novikov, M.A. Shifman, A.I. Vainshtein, V.I. Zakharov, Nucl. Phys. B **229**, 381 (1983)
68. M.A. Shifman, A.I. Vainshtein, Nucl. Phys. B **277**, 456 (1986) [Sov. Phys. JETP **64**, 428 (1986 ZETFA,91,723–744.1986)]
69. D.R.T. Jones, Phys. Lett. B **123**, 45 (1983)
70. J. Terning, Phys. Rev. Lett. **80**, 2517 (1998) [arXiv:hep-th/9706074]
71. F. Sannino, Acta Phys. Polon. B **40**, 3533 (2009) [arXiv:0911.0931 [hep-ph]]
72. F. Sannino, Phys. Rev. Lett. **105**, 232002 (2010) [arXiv:1007.0254 [hep-ph]]
73. V.A. Miransky, K. Yamawaki, Mod. Phys. Lett. A **4**, 129 (1989)
74. F. Sannino, arXiv:1205.4246 [hep-ph]
75. B. Holdom, Phys. Rev. D **24**, 1441 (1981)
76. B. Holdom, Phys. Lett. B **150**, 301 (1985)
77. T.W. Appelquist, D. Karabali, L.C.R. Wijewardhana, Phys. Rev. Lett. **57**, 957 (1986)
78. P. de Forcrand, M. Pepe, U.-J. Wiese, arXiv:1204.4913 [hep-lat]
79. F.A. Chishtie, V. Elias, V.A. Miransky, T.G. Steele, Prog. Theor. Phys. **104**, 603 (2000) [hep-ph/9905291]
80. F. Sannino, Phys. Rev. D **82**, 081701 (2010) [arXiv:1006.0207 [hep-lat]]

Springer

http://www.springer.com/978-3-642-33340-8

Dynamical Stabilization of the Fermi Scale
Towards a Composite Universe
Sannino, F.
2013, X, 124 p. 37 illus., 27 illus. in color., Softcover
ISBN: 978-3-642-33340-8